Journal Pre-proof

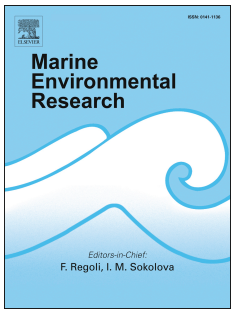

The arrival of a red invasive seaweed to a nutrient over-enriched estuary increases the spatial extent of macroalgal blooms

Ricardo Bermejo, Michéal MacMonagail, Svenja Heesch, Ana Mendes, Maeve Edwards, Owen Fenton, Kay Knöller, Eve Daly, Liam Morrison

PII: S0141-1136(19)30823-2

DOI: https://doi.org/10.1016/j.marenvres.2020.104944

Reference: MERE 104944

To appear in: *Marine Environmental Research*

Received Date: 9 December 2019

Revised Date: 25 February 2020

Accepted Date: 7 March 2020

Please cite this article as: Bermejo, R., MacMonagail, Miché., Heesch, S., Mendes, A., Edwards, M., Fenton, O., Knöller, K., Daly, E., Morrison, L., The arrival of a red invasive seaweed to a nutrient over-enriched estuary increases the spatial extent of macroalgal blooms, *Marine Environmental Research* (2020), doi: https://doi.org/10.1016/j.marenvres.2020.104944.

Ricardo Bermejo: Conceptualization, Methodology, Investigation, Formal analysis, Writing Original Draft, Project administration. **Michéal MacMonagail.**: Data curation, Investigation, Methodology, Writing- Original draft preparation. **Svenja Heesch**: Methodology, Visualization, Investigation. **Ana Mendes***:* Investigation. **Maeve Edwards**: Investigation. **Owen Fenton:** Investigation, Methodology. **Kay Knöeller:** Investigation, Methodology. **Eve Daly:** Resources, Funding acquisition, Supervision, Writing- Reviewing and Editing. **Liam Morrison:** Resources, Supervision, Writing-Reviewing and Editing, Funding acquisition.

Title: The arrival of a red invasive seaweed to a nutrient over-enriched estuary increases the spatial extent of macroalgal blooms.

Short title: Assessment and reconstruction of an *Agarophyton vermiculophyllum* (Gracilariales, Rhodophyta) invasion in a nutrient over-enriched Irish estuary.

Ricardo Bermejo[1*], Michéal MacMonagail[1], Svenja Heesch[2,3], Ana Mendes[1], Maeve Edwards[4], Owen Fenton[5], Kay Knöller[6], Eve Daly[1], Liam Morrison[1**].

[1] Earth and Ocean Sciences, School of Natural Sciences and Ryan Institute, National University of Ireland, Galway, H91 TK33, Ireland.
[2] UMR 8227- Integrative Biology of Marine Models, CNRS, Station Biologique de Roscoff, Roscoff, France.
[3] Institute for Biological Sciences, University of Rostock, Albert-Einstein-Straße 3, D-18059 Rostock, Germany.
[4] Zoology Department, School of Natural Sciences and Ryan Institute, National University of Ireland, Galway, H91 TK33, Ireland.
[5] Teagasc, Johnstown Castle, Co. Wexford, Ireland.
[6] Department of Catchment Hydrology, Helmholtz-Centre for Environmental Research - UFZ Theodor-Lieser-Straße 4, D-06120 Halle, Germany.

Corresponding authors:

*Ricardo Bermejo
email: ricardo.bermejo@uca.es
Tel: +353 (0)91 493200
ORCID: 0000-0003-3838-9093

**Liam Morrison,
email: liam.morrsion@nuigalway.ie
Tel: +353 (0)91 493200
ORCID: 0000-0002-8106-9063

ABSTRACT

The red seaweed *Agarophyton vermiculophyllum* is an invasive species native to the north-west Pacific, which has proliferated in temperate estuaries of Europe, North America and Africa. Combining molecular identification tools, historical satellite imagery and one-year seasonal monitoring of biomass and environmental conditions, the presence of *A. vermiculophyllum* was confirmed, and the invasion was assessed and reconstructed. The analysis of satellite imagery identified the first bloom in 2014 and revealed that *A. vermiculophyllum* is capable of thriving in areas, where native bloom-forming species cannot, increasing the size of blooms (ca. 10%). The high biomass found during the peak bloom (>2 kg m^{-2}) and the observation of anoxic events indicated deleterious effects. The monitoring of environmental conditions and biomass variability suggests an essential role of light, temperature and phosphorous in bloom development. The introduction of this species could be considered a threat for local biodiversity and ecosystem functioning in a global change context.

Keywords: *Gracilaria vermiculophylla*, *Agarophyton vermiculophyllum*, macroalgal bloom, satellite imagery, invasion, invasive seaweed.

Acknowledgements

This research was financed through the 2014-2020 EPA Research Strategy (Environmental Protection Agency, Ireland), project no: 2015-W-MS-20 (the Sea-MAT Project) and project no: 2018-W-MS-32 (the MACRO-MAN Project). The authors are thankful to Moya O'Donnell, Maria Galindo-Ponce, Claudia Cara-Ortega, Charlene Linderhof, Nichole Keogh, Andrew Niven and Edna Curley for field assistance and Robert Wilkes for advice and ground truthing images of the Clonakilty estuary from June 2013, July 2014 and August 2015. We appreciate the comments and review of the manuscript by Professor Ignacio Hernández.

1. Introduction

Estuarine environments harbour a great variety of habitats (e.g., seagrass meadows, salt marshes, oyster beds, mudflats) and are highly productive, providing valuable ecosystem goods and services (Costanza et al. 1997). Despite this variety of habitats and high biological productivity, species richness is relatively low due to the environmental fluctuations occurring over short spatial and temporal scales, which present a physiological challenge for the organisms inhabiting these areas (Jaspers et al. 2011; Cardoso et al. 2012; Bermejo et al. 2019b). In the case of macroalgae, the scarcity of hard substrates for the settlement of its propagules poses an additional constraint precluding the development of diverse seaweed assemblages. This absence of a suitable substratum is one of the main reasons why these environments have been traditionally less studied by phycologists (Krueger-Hadfield et al. 2017b, 2018).

Coastal ecosystems have been under strong and diverse anthropogenic pressures (e.g., nutrient enrichment, introduction of alien species, inputs of organic or inorganic contaminants), as human populations have historically been concentrated in these areas (Lotze et al. 2006; Airoldi and Beck 2007). These pressures can change the aquatic conditions producing different forms of pollution (e.g., dystrophy caused by an excess of eutrophication, biological invasions, and pollution by organic compounds and organic matter) that degrade the environment. Estuarine environments are more susceptible to over-enrichment of nutrients and other pollutants derived from human activity as a consequence of their hydrological and geomorphological characteristics (i.e., relatively small water bodies with low rates of water renewal). The combination of strong anthropogenic pressures and low species richness make these areas prone to successful biological invasions (Occhipinti-Ambrogi 2001).

One of the most evident signs of nutrient enrichment in estuaries is the development of opportunistic macroalgal blooms (Teichberg et al. 2010). These blooms are not toxic in and of themselves, but the accumulation and subsequent degradation of large amounts of seaweed biomass can produce deleterious consequences for the ecosystem and shore-based human activities (Sfriso et al. 2003; Smetacek and Zingone 2013). The development of macroalgal blooms has been traditionally attributed to nutrient over-enrichment of affected areas (Valiela et al. 1997; Smetacek and Zingone 2013). Although nutrient over-enrichment is a necessary requisite for the occurrence of seaweed blooms, other factors, such as temperature, light and salinity, are also crucial in explaining the development of these blooms (e.g., Malta and Verschuure 1997; Valiela et al. 1997; Gao et al. 2016). Previous studies suggested that the number of bloom-forming species in a particular area can also stimulate or prolong

the intensity, spatial extension and duration of the bloom, since temporal and spatial successions can occur (Lavery et al. 1991; Nelson et al. 2008; Bermejo et al. 2019a). The arrival of alien species with differing ecophysiological requirements can increase the potential for bloom occurrences in areas or periods of the year unfavourable for the blooming of native species. For instance, the arrival of non-native cryptic *Ulva* species has explained the development of seaweed blooms in two Japanese estuaries, where nutrients conditions have remained more or less constant (Yabe et al. 2009; Yoshida et al. 2015).

Due to difficulties in the identification of bloom-forming seaweeds (Steentoft et al. 1995; Malta et al. 1999; Rueness 2005) and the scarcity of phycological research in estuarine environments (Krueger-Hadfield et al. 2017b, 2018), species composition of macroalgal blooms and its importance for their development have been frequently overlooked. The development of new molecular identification tools allows researchers to overcome these taxonomic challenges, confirming the presence of seaweed blooms formed by cryptic alien species (e.g., Rueness 2005; Baamonde-López et al. 2007; Yoshida et al. 2015). In estuarine environments of North America, Europe and North Africa, such tools have verified the extensive spreading of the Asian red seaweed *Agarophyton vermiculophyllum* (Ohmi) Gurgel, J.N.Norris et Federicq (previously known as *Gracilaria vermiculophylla* (Ohmi) Papenfuss) (Kim et al. 2010; Krueger-Hadfield et al. 2017a). This gracilarioid can thrive in mudflats, as it remains anchored to the substrate by the burial of its basal parts, or attached to small pebbles or the shells of calcareous organisms. This species is also very resistant to different environmental stresses, such as low salinities, low light conditions or high grazing pressures (Nejrud and Pedersen 2010; Nylund et al., 2011), and it can bloom in areas, where native seaweeds cannot, modifying native biological assemblages and biogeochemical cycles in soft-sediment habitats (Byers et al. 2012; Cacabelos et al. 2012; Ramus et al. 2017).

The use of free, open-access satellite imagery has become a useful tool in the monitoring and assessment of macroalgal blooms (Hu et al. 2019; Zhang et al. 2019). Landsat-7 Enhanced Thematic Mapper Plus (L7-ETM+) provides satellite data from 1999 to the present, and this has been successfully used in identifying changes in marine environments (Andréfouët et al. 2001) and in mapping cyanobacterial bloom events (Vincent et al. 2004; Kutser et al. 2006). In comparison to L7-ETM+, the more recent Sentinel-2 Multispectral Instrument (S2-MSI) launched in June 2015 by the European Space Agency (ESA), delivers higher spectral (12 bands vs. 8 bands), spatial (10m vs. 30m) and temporal resolution data (2-day vs. 16-day revisit). These improvements have allowed the study of environmental processes occurring at smaller

temporal and spatial scales and have already been successfully used in the study of seaweed blooms (Xing et al. 2017, Dogliotti et al. 2018).

The identification of the most relevant temporal and spatial scales of variability is useful for understanding the factors controlling the abundance, distribution and composition of benthic assemblages (Burrows et al. 2009; Bermejo et al. 2015, 2019a). The assessment of the most relevant scales of variability is considered a necessary prerequisite before explanatory models are proposed (Andrew and Mapstone 1987). Furthermore, the use of exploratory correlational approaches can provide a general insight to help identify the primary environmental drivers controlling biomass development in the field (e.g., Malta and Verschuure 1997; Mac Nally 2002; Yoshida et al. 2015). The combination of both approaches improves the interpretation of the data collected.

The three objectives of this study were: to confirm the presence of *A. vermiculophyllum* in the Republic of Ireland using molecular identification tools, following a previous confirmation from Northern Ireland based on genetic identification (Krueger-Hadfield et al. 2017b); test the capability of free satellite imagery for the reconstruction of the invasion of this red alien species and its interaction with native species; elucidate the most important factors determining the development of the *Agarophyton* bloom in the Clonakilty estuary using an assessment of the spatial and temporal scales of variation combined with a correlational analysis of abiotic variables and biotic bloom conditions.

2. Material and Methods

2.1. Study site and Agarophyton identification based on molecular tools

The Clonakilty estuary is located on the southwestern coast of Ireland (Fig. 1) and has been historically affected by large intertidal macroalgal blooms formed by native *Ulva* spp. (Wan et al. 2017; Fort et al. 2020). This estuary is shallow, sheltered, and nutrient-enriched due to diverse human activities occurring in the surrounding area (i.e., intensive dairy farming and agriculture, the presence of a wastewater treatment facility). The Clonakilty estuary covers a surface area of 2.15 km^2 and has a length of 3.5 km. The residence time is between 6 and 9 days, the median depth is 2.5 m, and the estuary has a tidal range of 3.7 m. The studied areas affected by the *Agarophyton vermiculophyllum* bloom were muddy (percentage of fine sand and clay between 65 and 97%; Lewis et al. 2002) and enriched in organic matter (between 2.5 and 7%;

nitrogen content between 0.05 and 0.25%). The bay is sheltered and protected from wave exposure.

2.2. Environmental conditions

Daily climatological data for Clonakilty (i.e., rainfall, maximum and minimum air temperature) were obtained from the Irish meteorological service (Met Éireann; http://www.met.ie/). Rainfall data were sourced from the closest pluviometric station in Rosscarberry (20 km). The maximum and minimum air temperature levels were linearly interpolated considering the distance from the sampling site to the two closest meteorological stations of Sherkin Island and Roche's Point, which were located 40 and 48 kms respectively from the study site. Each parameter (i.e., accumulated rainfall, solar radiation and maximum and minimum air temperatures) was calculated considering data from the week previous to each sampling occasion.

Seawater sampling for physicochemical variables (i.e., salinity and dissolved inorganic nutrients) was conducted during the previous or subsequent high-tide following the biomass sampling over six occasions (i.e., data from July 2016 were not collected due to logistical reasons). Seawater samples were collected from each sampling site at a depth of 20 cm (Fig. 1). Salinity was determined *in situ* using a hand refractometer (ATAGO S-20E, Tokyo, Japan). Three replicate samples of water were collected for the determination of dissolved inorganic nutrients (nitrate, nitrite, ammonium and phosphate). Replicates were filtered *in situ* using a syringe and a nylon disposable filter (pore size 0.45 µm; Sarstedt, Germany) and samples were stored at -20ºC prior to analysis. Seawater samples analysed for total oxidised N (TON) concentrations were determined on a Thermo Aquakem discrete analyser (Thermo Scientific, Vantaa, Finland), with a detection limit of 0.25 mg L^{-1} for total oxidised N. Samples were also analysed for NO_2−N, $NH4^+$-N, and dissolved reactive phosphorus (DRP) on the same instrument and Nitrate-N (NO_3-N) was calculated by subtracting NO_2−N from TON.

2.3. Agarophyton identification based on molecular tools

The red alga thriving on the intertidal mudflats of the Clonakilty estuary was identified at species level using a plastid-encoded marker, the large subunit of the Ribulose Bisphosphate Carboxylase-Oxygenase (RuBisCO) (*rbc*L). This marker is widely used to unravel taxonomical issues within the phylum Rhodophyta, providing sufficient variation for species delimitation in conflicting taxa (Freshwater and Rueness 1994; Rueness 2005; Guillemin *et al.* 2008), and it confirmed the first record of

Agarophyton vermiculophyllum for Europe (Rueness 2005). Algal tissue was dried with desiccated silica (see section 2.5 for details), and whole genomic DNA was extracted with a commercial kit [NucleoSpin® Plant II, Macherey-Nagel, Düren, Germany]. Amplifications of the *rbc*L gene region in Polymerase Chain Reactions (PCRs) employed primers F8 or F57, and R1150 (Mineur et al. 2010; Freshwater and Rueness 1994) at an annealing temperature of 50ºC (Heesch et al. 2009). Protocols for PCR amplification, purification of the products and sequencing followed Heesch et al. (2016).

Six sequences from Clonakilty specimens were aligned with 57 published Gracilariacean sequences from all over the world (including *A. vermiculophyllum* sequences from Asia and USA, e.g., JQ407698, JQ768761, DQ095821, EU600293), using sequences of the genus *Hydropuntia* (JQ843362 and EF434914) as an outgroup. Methods for the treatment of sequences (i.e., quality control and alignment) and the analyses of data under the Maximum Likelihood (ML) criterion are given in Heesch et al. (2016). The algal nomenclature followed AlgaeBase (Guiry and Guiry 2019). Representative herbarium specimens were deposited at GALW under accession numbers GALW01650-GALW01652.

2.4. Reconstruction of Agarophyton invasion and assessment of the biotic interaction with native species using satellite imagery

In order to reconstruct the arrival of *A. vermiculophyllum* and assess the potential spatial overlapping of this invasive red alga with the native bloom-forming species *Ulva* spp. in Clonakilty Bay, two sources of free satellite data were used, namely the MultiSpectral Instrument onboard Sentinel-2 (S2-MSI) and the Landsat-7 Enhanced Thematic Mapper Plus (L7-ETM+). Suitable data scenes from 2010-2018 captured during bloom proliferation (April-September), at low tide and on cloud-free days, were initially identified using Google Earth Engine (GEE; Gorelick et al. 2017). The earliest S2-MSI scenes available of the study area were from July 2015, and prior to this date, L7-ETM+ data were used. Both Level-2A and Level-1C S2-MSI scenes from 2015-2018 were downloaded from the Copernicus DataHub website (https://scihub.copernicus.eu/), and L7-ETM+ data from 2010 – 2014 from the United States Geological Survey (USGS) website (https://earthexplorer.usgs.gov/). From 2015 – 2018, S2-MSI was used instead of L7-ETM+ because of the improved revisit time and spectral resolution, which allowed for improved classification of *Ulva* spp. and *A. vermiculophyllum*. To avoid any bias in spatial resolution and allow comparison

between the datasets, both downloaded L7-ETM+ and S2-MSI scenes were resampled to 30 m spatial resolution.

Initial processing of both satellite products was carried out using the European Space Agency (ESA) Sentinel Application Platform (SNAP) toolbox (v. 6.0). Both datasets were geometrically rectified to Universal Transverse Mercator (UTM) zone 29N projection and WGS 84 datum. True colour composite images of the study area were created by combining, in the case of S2-MSI, the B2: blue (490 nm), B3: green (560 nm) and B4: red (665 nm), and for L7-ETM+ the B1: blue (450 nm), B2: green (520 nm) and B3: red (630 nm). Further processing, including atmospheric and radiometric corrections using SNAP Desktop and ENVI software (v. 5.3.1; Research Systems, Boulder, CO, US). Sentinel-2 Level-1C and L7-ETM+ radiance data recorded at the top of atmosphere (TOA) were scaled to surface reflectance by applying the dark object subtraction (DOS) technique (Gilmore et al. 2015), before atmospheric correction to Level-2A bottom of atmosphere (BOA) data using Sen2Cor (Louis et al. 2016).

A pixel-based maximum likelihood classifier (MLC) was applied to individual corrected scenes to produce both *Ulva* spp. and *A. vermiculophyllum* masks. The MLC function is available in the ENVI software and calculates the average variance of the spectral training data to estimate the likelihood of a pixel belonging to each class (Foody 1992). The MLC was based on pixel training with >200 pixels per class used to train the data. Superfluous classes (water, terrestrial and saltmarsh vegetation, sand) were masked from each scene and later removed before images were refined and smoothed to improve image sharpness. The total accuracy and the kappa coefficient (Cohen 1960) of the classification were also calculated.

The annual cover, potential extension and overlapping between native and invasive bloom-forming species were estimated using QGIS (Quantum GIS Development Team 2014, Quantum GIS Geographic Information System, Open Source Geospatial Foundation Project, http://qgis.osgeo.org). In this study, the potential extension of both *A. vermiculophyllum* or *Ulva* spp. was defined as the entire area covered by these species at least once during the study period. A workflow showing the overall processing of the satellite imagery is shown in Figure S1.

2.5. Biomass sampling and processing

To infer the most important factors influencing the development of *A. vermiculophyllum* blooms, the estuary was sampled on seven sampling occasions between July 2016 and August 2017. Biomass sampling was conducted during low

water conditions of the spring tides. On each sampling occasion, a hierarchical design was followed to identify the most relevant scales of spatial variation in *Agarophyton* biomass. Two sections ("inner" and "outer") covered by large *Agarophyton* patches and separated by two kilometres were sampled (Fig. 1 a and b). In each section, two sites separated by one hundred meters were selected. In one site per section, two random transects perpendicular to the main channel and separated by 10 meters were sampled. In the second site, only one random transect was sampled. Along each transect, three sampling stations were positioned in the upper (between 2.4 and 2.1 m above Mean Lower-Low Water -MLLW-), middle (between 2.0 and 1.8 m above MLLW) and lower (between 1.7 and 1.4 m above MLLW) part of the intertidal covered by the bloom during their maximum extension. The maximum extension usually occurs in June or July in cold-temperate North Atlantic estuaries (e.g., Thomsen et al. 2006; Weinberger et al. 2008; Sfriso et al. 2012; Surget et al. 2017). The sampling stations were pre-determined using Sentinel-2 images of bloom events from 2015. The pre-defined sampling stations were located in the field using a Geographical Position System (GPS; Magellan Triton 400, Santa Clara, USA). Sampling stations differed in locations between sampling occasions to avoid the confounding effect of destructive resampling. At each sampling station (eighteen sampling stations per occasion), three quadrats (25 x 25 cm) were used to assess the abundance of seaweed. All living material present in each quadrat was collected, placed in labelled plastic bags and transported to the laboratory.

Once in the lab, the seaweed biomass was rinsed with fresh water to remove adherent sedimentary and particulate material, debris and other organisms. Seaweed species were sorted, and their mass was recorded after the removal of excess water using a manually operated low-speed centrifuge (i.e., salad spinner). Three subsamples of seaweed biomass per section and sampling occasion were rinsed with deionised water, freeze-dried and stored in a desiccator until further elemental analysis (i.e., tissue N and P content). Furthermore, some specimens were washed with deionised water and stored in dry silica gel for taxonomic identification.

2.6. Tissue nutrient (N and P) analyses

Nitrogen and phosphorus are considered the main nutrients limiting primary production in aquatic environments. Overall, nitrogen has been traditionally considered to play a more important role in controlling maximum bloom development in coastal systems (Valiela et al. 1997). Nevertheless, phosphorus has also been identified as a limiting nutrient in cold temperate estuaries during periods of the year (Pedersen and

Borum, 1996; Lyngby et al. 1999), and even different species can be limited by nitrogen or phosphorous in the same estuary (Lavery et al. 1991; Villares and Carballeira 2004). In order to identify nitrogen or phosphorus limitation, it is necessary to estimate the tissue nitrogen and phosphorus contents and compare with the critical quota, which provides a direct measure of the nutrient status of seaweed. The critical quota is the minimum tissue nutrient content necessary to support unrestrained growth by the lack of nutrients. In the case of *A. vermiculophyllum*, the critical quota for nitrogen (2.14 % DW) and phosphorous (0.14% DW) have been previously determined by Pedersen and Johnsen (2017).

Seaweed tissue, previously freeze-dried, was ground into a homogeneous powder using a TissueLyser II (QIAGEN) and tungsten balls. The homogenised sample was divided into two subsamples; one was used for N and the other for P determination. To determine tissue N content, aliquots of the homogenised material were weighed into tin capsules that were combusted in an elemental analyser Vario ISOTOPE Cube (Elementar Analysensysteme GmbH, Hanau) connected to an isotope ratio mass spectrometer Isoprime 100 (Isoprime Ltd, Cheadle Hulm). The analytical precision was 0.15%. Analyses were carried out in duplicates. Tissue P content was determined on the same dried and ground seaweed tissue after oxidation with boiling H_2SO_4 followed by spectrophotometric analysis (Strickland and Parsons, 1968).

2.7. Statistical analyses

Statistical analyses were performed using the R free software environment (R Core Development Team, 2017) and PERMANOVA+ add-on PRIMER 6 (Plymouth Routines in Multivariate Ecological Research) software. In all statistical analyses, significance was set at 5% risk error, and when necessary were based on 5999 permutations.

2.7.1. Spatial and temporal patterns of variation

To identify the relevant spatial and temporal scales of biomass distribution of *A. vermiculophyllum*, a univariate five-way permutational analysis of variance (PERMANOVA; Anderson et al. 2008) was performed based on the Euclidean distances. The five factors considered (three fixed and two random) were: Sampling occasion (fixed; seven levels: "July 16", "August 16", "October 16", "February 17", "April 17", "June 17", and "August 17"), Position in the bloom (fixed; three levels: "upper", "middle" and "lower"), Section (fixed: "Inner" and "Outer"), Site (random; two levels nested in the interaction between "Section" and "Sampling occasion"), and

Sampling station (random; two levels nested in the interaction between "Site" and "Position"). In the case of significant effects of a fixed factor, a pairwise PERMANOVA test (Anderson et al. 2008) was performed in order to interpret the patterns. Biomass data complied with homoscedasticity in accordance with the Levene test, but not with normality according to the Shapiro-Wilks test.

A two-way factorial ANOVA design was considered to assess the effects of "Sampling occasion" (seven levels) and "Section" (two levels) on tissue N and P content of *A. vermiculophyllum*. Tissue N and P content data can be considered normal and homoscedastic in acordance with Shapiro-Wilks and Levenes tests. A Tukey's test was used to compare levels of factors when an effect was significant.

2.7.2. Correlations between biotic and environmental variables

To interpret and visualise the relationships between environmental variables and the *Agarophyton* bloom in Clonakilty, correlations between environmental variables (i.e., dissolved inorganic nutrients, salinity, radiation, rainfall, and maximum and minimum air temperatures) and biotic variables (i.e., mean *Agarophyton* biomass, mean tissue N and P content, and mean N:P ratio) were assessed using Spearman correlations (Rho), and a principal component analysis. The principal component analysis (PCA) was based on biotic variables, and environmental variables were fitted later using the "envfit" function of the "Vegan" package in R (R Core Development Team, 2017). To perform these analyses, data from the four sampling sites and six of the seven sampling occasions were considered (n=24), as water physicochemical attributes from June 2016 were absent.

3. Results

3.1. Environmental conditions

Climatological conditions are shown in Table 1. Solar radiation and maximum and minimum air temperatures were highest in June and August as expected for a temperate estuary in the Northern Hemisphere. The maximum air temperature during the week before the sampling varied from 12.3ºC (April 2017) to 26.0 (June 2017), and the minimum air temperature from 2.0ºC (April 2017) to 12.6 (August 2016). Mean daily radiation ranged from 401.2 (February 2017) to 1587.0 (June 2017) J cm^{-2}. The accumulated rainfall during the week previous to the sampling occasion was minimum in October 2016 and April 2017, and maximum in July 2016 and August 2017.

The physicochemical water characteristics are presented in Table 2. Nitrate was the main source of DIN, followed by ammonium. Total DIN concentrations ranged from 10 (Site "Outer 2"; April 2017) to 285.71 µM DIN (Site "Inner 1"; February 2017). Overall, the maximum DIN concentrations were observed in October 2016, with the exception of Site 1. The DIP (dissolved inorganic phosphate) concentration varied between 0.16 (Site "Outer 1"; April 2017) and 1.99 µM DIP (Site "Inner 1"; August 2017). Inner sites exhibited higher nutrient concentrations than sites located in the outer part of the estuary. Regarding salinity, the value ranged between 5.0 (Site "Inner 1"; June 2017) to 33.2 (Site "Outer 2"; October 2016).

3.2. Taxonomical confirmation based on molecular tools

The *rbc*L marker was amplified in six specimens of gracilarioids from the Clonakilty estuary. Sequences were included in an alignment of 1419 bases length, containing 67 sequences in total, with *Hydropuntia* Montagne species serving as outgroup. The Irish specimens (GenBank/ENA accession numbers LR740737-LR740742) were identified as belonging to the species *Agarophyton vermiculophyllum* (order Gracilariales; Fig S1). Additionally, three other red algal species were observed in the estuary, albeit as drift material with low biomass, which were identified based only on morphological traits: *Gracilariopsis longissima* (S.G.Gmelin) Steentoft et al., *Gracilaria gracilis* (Stackhouse) Steentoft et al. and *Cystoclonium purpureum* (Hudson) Batters.

3.3. Reconstructing the invasion and assessing the overlap with native bloom-forming species.

The pixel-based MLC resulted in satisfactory overall accuracy with the kappa coefficient ranging from 0.7317 to 0.9617 when compared with manual classification (Table 3). A time-series of images (2010-2018) plotting the extension of both blooms during peak proliferation are presented in Figure S3. In the case of *Ulva*, the total extension of the bloom ranged from 19.6 (2013) to 50.8 (2015) ha between 2010 and 2018, although some caution should be exercised when comparing among years due to data acquisition in different months of the year (Table 3). The analysis of the satellite imagery identified 2014 as the year when the *A. vermiculophyllum* bloom first appeared in Clonakilty Bay. The encroaching *A. vermiculophyllum* canopy is evident from 2014 to 2018 when the area colonised increased from 3.9 to 8.1 ha (Table 3; Fig. S2). The spatial comparison between the potential extensions of *Ulva* spp. (63.1 ha) and *A. vermiculophyllum* (9.9 ha) revealed an increased overlapping from 2015 to 2018

between the native green algae and the invasive red alga due to the colonisation of *Agarophyton* in areas potentially covered by *Ulva* (Table 3). The results showed that *A. vermiculophyllum* colonised the northern shore, which had remained relatively bloom-free prior to 2014 (Fig. 2). The total extension of the estuary potentially covered by bloom-forming species of both *A. vermiculophyllum* and *Ulva* spp., increased by 6.7 ha after the arrival of *A. vermiculophyllum*. In this sense, the average size of macroalgal blooms during peak bloom conditions was 1.21 times larger during the period 2014-2018 (39.6 ha) than for the period from 2010-2013 (32.7 ha).

3.4. Spatial and temporal patterns of variation

The PERMANOVA results regarding the biomass of *A. vermiculophyllum* revealed significant differences among sampling occasions, sections and positions (Table 4). A common seasonal dynamic in the biomass of *Agarophyton* was observed in both inner and outer sections, with annual peaks of biomass during summer, between June and August (Fig. 3a), and minimum levels detected in winter (i.e., February 2017). Overall, higher biomasses of *A. vermiculophyllum* were observed in the inner section than in the outer, except during April 2017, when the opposite trend was recorded. The annual peaks of biomass occurred in July 2016 and in August 2017 for both sections. The mean values observed in the inner section during July 2016, and August 2017 were 2.41 and 1.88 kg FW m^{-2}, respectively, reaching abundances higher than 5.00 kg FW m^{-2} at some sampling stations. In the outer section, the mean values observed during the peak bloom were 1.15 and 1.52 kg FW m^{-2} for July 2016 and August 2017, reaching abundances greater than 2.50 kg FW m^{-2} during this period. In contrast, during February 2017, the mean values of biomass were 229.8 g FW m^{-2} and 229.0 g FW m^{-2} for the inner and outer sections.

Regarding the shore position of the *A. vermiculophyllum* bloom, the middle position reached higher biomass abundances than the lower position (Fig. 3b). This pattern is dependent on the "Section" and "Site", as revealed by the significant interaction between "Position" and "Section", and also "Position" and "Site" (Table 4). However, this pattern was evident in the inner section, but not in the outer, as shown in Figure 3b. Finally, at smaller spatial scales of variation, significant differences were observed between sites, but not between sampling stations (Table 4). The low data dispersion within sampling stations indicates homogeneity in biomass distribution at small spatial scales (Fig. S3).

In relation to the tissue N content, the ANOVA revealed significant differences between sampling occasions, but not between sections (Table 5). No significant

interactions between "Sampling Occasion" and "Section" were found. The tissue N content followed a seasonal pattern, opposite to the one observed for biomass abundance (Fig. 4a). The maximum percentage of tissue N occurred in February (4.68±0.31%; mean±SD, n =6), coinciding with minimum biomass abundance, and the minimum percentage of tissue N content was found during the summer (July 2016; 2.27±0.36%; n =6), coinciding with maximum biomass. In the case of the tissue P content, the ANOVA revealed significant differences between sampling occasions, and a significant interaction between "Sampling Occasion" and "Section" (Table 5). Both sections displayed a relatively similar seasonal trend with maximum tissue P contents during February 2017 and minimum levels in April and June 2017 (Fig. 4b). In the inner section, the lowest tissue P content was observed in June 2017 (0.093±0.009 %; n=3), and the highest contents in August 2016 (0.173±0.037 %; n=3) and February 2017 (0.178±0.041 %; n=3). In the outer section, the lowest tissue P contents were observed in April (0.082±0.005 %; n=3) and June 2017 (0.087±0.006 %; n=3), and the highest contents in October 2016 (0.203±0.039 %; n=3) and February 2017 (0.193±0.026 %; n=3).

3.5. Correlations between biomass and environmental variables

The first two components of the PCA based on biotic variables explained over 94.2% of the total variation (Fig. 5). The score plot showed three main clusters, one grouping data from October 2016 and February 2017 characterised by high tissue nutrient contents and low biomasses, a second cluster including April and June 2017 with relatively high biomasses and tissue N:P ratios due to low tissue P contents, and a third cluster with samples from August 2016 and 2017, which displayed high biomass and low N:P ratios as a consequence of an increase in tissue P contents.

The "envfit" function and Spearman correlations between biotic and environmental variables suggested an important effect of light (i.e., solar radiation) and temperature (i.e., maximum and minimum air temperatures) on the biological performance of *A. vermiculophyllum* (i.e., tissue N and P contents, N:P ratio and Biomass) (Table 6 and Fig. 5). The "envfit" found significant correlations with biotic variables for DIN (r^2 =0.283; p-value <0.05), radiation (r^2=0.727; p-value<0.001), maximum (r^2=0.517; p-value<0.01) and minimum (r^2=0.639; p-value<0.001) temperatures, and marginal correlations for Salinity (r^2=0.225; p-value<0.10). The Spearman correlations (Table 6) indicated that biomass was significantly and positively correlated with radiation, and maximum and minimum temperatures, and negatively correlated with salinity and DIN concentration (Rho=-0.39; p-value <0.10). Tissue N content was positively correlated

with DIN concentration, and exhibited negative and significant correlations with temperatures and solar radiation. In the case of tissue P content, only radiation showed a negative and significant correlation (Rho =-0.61; p-value <0.01). The tissue N:P ratio was significantly and negatively correlated with maximum and minimum temperatures. Biomass was significantly and negatively correlated with tissue N content (Rho =- 0.76; p-value <0.001), and tissue N:P ratio (Rho=-0.50: p-value <0.01), but did not show any correlation with tissue P content (Rho=-0.18; p-value >0.10).

4. Discussion

Molecular genetic identification confirmed the presence of *A. vermiculophyllum* in the Republic of Ireland for the first time, which had previously been recorded from Northern Ireland (UK) (Krueger-Hadfield et al. 2017b). In the Clonakilty estuary, the use of satellite data identified 2014 as the first year, when *A. vermiculophyllum* produced a bloom, and confirmed, that this species can bloom in areas of the estuary devoid of native macrophytes. The assessment of the most relevant scales of variability revealed a clear seasonal pattern, with maximum biomass abundance during summer and minimum levels in winter. Similar seasonal trends were observed in other cold-temperate estuaries (e.g., Weinberger et al. 2008; Muangmai et al. 2014; Surget et al. 2017). Regarding the most relevant scales of spatial variability, the analysis revealed significant variability between sections, sites and positions within the bloom, but not between sampling stations, suggesting homogeneity at small spatial scales. The high tissue N contents observed (>2%) suggests that *A. vermiculophyllum* is not limited by nitrogen at any time of the year since these values were higher than the critical quota (2.14%) proposed for this species by Pedersen and Johnsen (2017). The positive correlation of DIP with biomass (Rho =0.33; p-value=0.11), and the fact that tissue P contents were below the critical quota (0.14%) during the period of active growth (from February to June) indicated that *Agarophyton* could be limited by P. The correlations and PCA analyses indicated that temperature and photoperiod are essential factors controlling the potential development of *A. vermiculophyllum* biomass in Irish estuaries.

4.1. Presence of A. vermiculophyllum confirmed in the Republic of Ireland

In this study, the presence of *A. vermiculophyllum* in the Republic of Ireland is confirmed based on molecular evidence. Evidence has suggested oyster cultures as the main vector for the introduction and spread of this species in European and

American estuaries (Krueger-Hadfield et al. 2017a). Although no oyster aquaculture facilities occur in Clonakilty Bay, oyster farming is present in other nearby estuaries, such as Oysterhaven (approx. 30 kilometres East following the coastline) and Roaringwater Bay (approx. 50 kilometres West). This species was also recorded from the adjacent Argideen estuary based on morphological identification, where this species might be present in relatively low abundance (Bermejo et al. 2019a). Considering the geographical location of this record from the southernmost Irish coast (i.e., Clonakilty), along with the ubiquity of oyster cultivation throughout Ireland (https://www.agriculture.gov.ie/), it is very likely that this species is more wide spread along the Irish coast than currently known. The secondary spreading of this species from estuaries, where oyster cultures are established, could explain the presence of *A. vermiculophyllum* in Clonakilty. As this red alga can survive under harsh environmental conditions (Nyberg and Wallentinus 2009) and possesses a high vegetative dispersal potential (Krueger-Hadfield et al., 2016; Surget et al. 2017), it can be easily transported from one estuary to another entangled in fishing nets, boat anchors, by migrating birds or by coastal currents as drift material (Nyberg and Wallentinus 2009; Martínez-Garrido et al. 2017).

4.2. A new opportunistic species blooming in areas where native opportunistic species cannot

The red seaweed *Agarophyton vermiculophyllum* is known to be more tolerant to different stresses (e.g., desiccation, extreme temperatures and salinities) and to thrive in a wide range of environmental conditions, displaying relatively fast growth rates (Abreu et al. 2011; Pedersen and Johnsen 2017). This species is considered a euryhaline species, performing best under mesohaline conditions (optimal salinity between 10 and 20; Rueness, 2005; Weinberger et al., 2008), being more competitive than *Ulva* in areas under variable salinity conditions (Sfriso et al., 2012). Moreover, *A. vermiculophyllum* also exhibits chemical defences that make it less affected by grazing and subsequently being less consumed in invaded areas than native species (Nylund et al. 2011; Rempt et al. 2012). As a consequence of the relatively fast growth of *A. vermiculophyllum* combined with its ecological performance, and probably linked to concurrent eutrophication processes, this species has outcompeted native macrophytes in some invaded estuaries (e.g., Nejrup and Pedersen 2010; Cacabelos et al. 2012; Sfriso et al. 2012; Thomsen et al. 2013), or has bloomed in areas previously devoid of other macrophytes (Byers et al. 2012; Ramus et al. 2017; Surget et al. 2017). In this case, the analysis of the satellite images pre- (from 2010 to 2013)

and post- (from 2014 to date) the *Agarophyton* bloom occurrence revealed some overlapping between *Ulva* spp. and *A. vermiculophyllum* blooms in the four years following the appearance of the first bloom (Figs. 2 and S2), but this invasive species has also proliferated in areas of the Clonakilty estuary devoid of native macrophytes, where salinity is usually lower and more variable as consequence of freshwater inflows (Yokoya et al. 1999; Sotka et al., 2018). This leads to an overall larger area of the estuary affected by macroalgal blooms and to subsequent problems (e.g., summer anoxic events, odours), but also in a greater area capable of retaining large amounts of nutrients during late spring and summer, when temperature and light conditions are favourable for the development of even more potentially harmful microalgal blooms (Sverdrup 1953).

These results have also revealed that the analysis of free open-access satellite imagery can be a useful and powerful tool to track recent biological invasions of conspicuous species in intertidal environments. The L7-ETM+ provided an interesting data record from 1999 to date and allowed the assessment of the potential area affected by macroalgal blooms and the identification of the first *Agarophyton* bloom event in 2014. This first bloom observation was supported by data from the Irish Environmental Protection Agency from annual monitoring survey of this estuary in the context of the EU Water Framework Directive (R. Wilkes, pers. com.; Fig. S5). However, considerable limitations exist in the use of L7-ETM+ data as a result of the long revisit time (16-days) and excessive cloud coverage. The combination of these factors prevented any data acquisition from 2011 and precluded the comparison between years as imagery was not always available during the peak bloom period (June-August). The enhanced spatio-temporal resolution of the S2-MSI reduces these constraints. The higher revisit time of Sentinel-2 (2-days) improves the likelihood of detecting bloom events on cloud-free days. Furthermore, the higher spatial resolution of S2-MSI will improve the accuracy when studying estuarine bloom events similar in size to that found in Clonakilty.

4.3. Temporal variability

Biomass of *A. vermiculophyllum* was present throughout the year, showing clear seasonal dynamics, with annual peaks of biomass during the summer (July-August) and minimum biomass in winter (February), as observed in other cold-temperate regions (e.g., Thomsen et al. 2006; Weinberger et al. 2008; Muangmai et al. 2014). The highest values of biomass were observed in the inner section during July 2016 (mean±SD =1.78±1.11 kg FW m^{-2}; maximum =5.44 kg FW m^{-2}) and August 2017

(mean±SD =1.70±1.08 kg FW m^{-2}; maximum =5.21 kg FW m^{-2}). These maximum values were similar to those observed in other areas affected by *A. vermiculophyllum* blooms such as the Le Faou and Penfoul estuaries (France; 1.64 - 2.22 kg FW m^{-2} considering a 0.17 ratio dry: fresh weight; Surget et al. 2017), Mockhorn mudflat (northeast coast of USA; 1.67-2.28 kg FW m^{-2}; Gulbransen and Mcglathery 2013), Aveiro lagoon (Portugal, 2.37 kg FW m^{-2}; Abreu et al. 2011), or Holckenhavn Fjord (Denmark; 2.73 kg FW m^{-2}; Nejrup and Pedersen 2010), but lower than those observed in the Venice Lagoon (Italy) during conditions of peak biomass (6.53 kg FW m^{-2}; Sfriso et al. 2012).

The observed seasonal biomass dynamics was mainly explained by photoperiod and temperature, and the bloom size might be constrained by P rather than N limitation, as supported by the high tissue N contents observed throughout the year and the low tissue P contents observed during the season of active growth (from February to August; Figs. 3 and 4). The negative correlation between tissue N content and biomass (Rho =- 0.71; p-value <0.001) suggest a biomass dilution effect due to intensive growth during bloom development (Bermejo et al. 2019b). On the other hand, the positive correlation between DIP and biomass, and with tissue P contents below the critical quota (Pedersen and Johnsen 2017) supports the occurrence of P limitation during the period of intensive growth. Tissue P content seems to increase during the peak bloom (July 2016, and August 2016 and 2017; Figs. 3 and 5), likely a consequence of slower growth and a higher nutrient availability associated to an enhanced biomass degradation. The relative variation in biomass is positive and high from February to June (Fig. 3) as increasing temperatures and longer photoperiods promote the development of *A. vermiculophyllum*. After July, the higher temperatures might increase the stress during the desiccation period and enhance biomass degradation. In this sense, during August 2016 an anoxic event which was caused by the degradation of *Agarophyton* biomass was evident in the inner section of the Clonakilty estuary. In the outer section, the overgrowth of the bacterial community (observed as a milky liquid in the surface of the sediment or seaweeds) was not as evident or extensive. The hypoxic conditions and the release of toxic compounds (e.g., H_2S, NH_4^+, NO_2^-) associated with these events can cause stress (e.g., Vermaat and Sand-Jensen 1987; Grazia-Corradi et al. 2006) and result in the rapid decline of the *Agarophyton* biomass (Thomsen et al. 2006; Sfriso et al. 2012). The high concentrations of ammonium observed during peak biomass in the inner section, where summer anoxic events were evident, and the positive correlations between minimum air temperature, and NO_2^- (rho =0.4; p-value <0.1) and NH_4^+ (Rho =0.53; p-value <0.01), support this hypothesis (Table 2).

650

651 *4.4. Spatial variability*

652

653 Unattached specimens entrained in mudflat sediments mainly comprised the *A.*
654 *vermiculophyllum* bloom in the Clonakilty estuary. Nevertheless, sporophytes and
655 gametophytes were observed, and some specimens attached to small pebbles or
656 cockleshells were found in the outer section of the estuary, suggesting the existence of
657 non-vegetative reproduction (Krueger-Hadfield et al. 2016). The assessment of the
658 most relevant scales of variability (Table 4) indicated a homogeneous distribution at
659 scales of meters or tens of meters, with no differences between, and little data
660 dispersion within sampling stations. This can be explained by the low environmental
661 heterogeneity in these mudflats at small spatial scales, and because *Agarophyton*
662 remains somewhat anchored to the substrate by the burial of the basal part of the
663 thallus. This has relevant implications for the biomass distribution and transport of
664 macrophytes, determining biomass and nutrient balances in the estuary (Schories and
665 Reise 1993; Bermejo et al. 2019a). This entrainment in the sediment could also provide
666 access to nutrients from porewaters, as demonstrated in the case of *A. chilense*
667 C.J.Bird et al. (=*Gracilaria chilensis* (C.J.Bird et al.) Gurgel et al.), which is also
668 entrained in mudflat sediments from South Pacific estuarine environments (Robertson
669 and Savage 2018).
670 At larger spatial scales, significant differences were observed in *Agarophyton*
671 biomass distribution. Overall, higher seaweed biomass was found in the inner section,
672 where both higher dissolved nutrient concentrations (DIN and DIP) and lower salinities
673 were observed. This could favour the biological performance of *A. vermiculophyllum,*
674 according to previous ecological and physiological studies (Yokoya et al. 1999;
675 Rueness 2005; Weinberger et al. 2008). Considering the similar tissue N content found
676 in the inner and outer sections, and the high values observed during the peak bloom,
677 both lateral transport and export from the estuary by wind and tidal currents might
678 explain this biomass differences. Differences between positions within the bloom were
679 also observed. However, distribution patterns were not homogeneous between
680 sections and sites, suggesting different mechanisms may influence abundances in a
681 perpendicular gradient to the main channel (Figs. 3b and S3).
682 In rocky intertidal habitats, seaweed attachment combined with critical physical
683 factors, such as emersion time and wave exposure, results in clear zonation patterns
684 (Mangialajo et al. 2012; Chappuis et al. 2014). In mudflats, the lower slope, reduced
685 wave exposure and weaker attachment of macrophytes to the substrate result in less
686 evident and less consistent zonation patterns. In these areas, the distribution of

687 macrophytes weakly anchored to the sediment such as *Ulva* spp. or *Agarophyton*
688 might be the result of the effects of local environmental conditions on their biological
689 performance, but also the biomass transport due to winds, wave action and tidal
690 currents.
691
692 *4.5. Relevance for environmental management*
693
694 The arrival of *A. vermiculophyllum* to American and European estuaries has relevant
695 impacts on the ecological functioning of mudflats. Overall, this alga acts as a habitat-
696 forming species in areas previously devoid of vegetation for some organisms, thereby
697 increasing habitat complexity, enhancing epibenthic diversity and altering
698 environmental conditions (Wright et al., 2014; Davoult et al. 2017; Ramus et al. 2017).
699 In the context of eutrophication, the decay rate is slightly lower than alternative bloom-
700 forming *Ulva* spp., slowing down remineralisation cycling and acting as a temporal sink
701 for nutrients (Thomsen et al. 2007; Pedersen and Johnsen 2017). The presence of
702 *Agarophyton* increases net denitrification rates in comparison with bare sediments,
703 thus favouring the removal of nitrogen from the estuary (Gonzalez et al. 2013).
704 However, this species occupies mudflats, which are protected by the European Habitat
705 Directive (92/43/EEC; Habitat 1140). These mudflat habitats harbour their own unique
706 and diverse biota and play a key role in the life cycle of some specialised organisms,
707 such as shorebirds (Haram et al., 2018). Depending on the biomass density of this
708 habitat-forming species, some of the aspects observed by previous authors may have
709 ambiguous or deleterious effects on the environment. For instance, Gonzalez et al.
710 (2013) pointed out, that at high densities (approx. 700 gr FW m^{-2} *A. vermiculophyllum*)
711 denitrification rates dropped, suggesting a potential biomass threshold for macroalgal
712 enhancement of denitrification. Although the nutrient cycling may be slowed down
713 when fast-growing species like *Ulva* spp. are replaced by *Agarophyton*, the opposite is
714 expected when *A. vermiculophyllum* is replacing slow-growing species such as *Fucus*
715 spp., *Ascophyllum nodosum* or seagrasses (Pedersen and Johnsen 2017). The
716 occurrence of summer anoxic events and associated massive mortalities of epifauna
717 and infauna should also be considered (Mineur et al., 2015; Ramus et al., 2017; Keller
718 et al. 2019). Such anoxic events due to excessive input of organic matter by
719 decomposing *Agarophyton* biomass has been described before (e.g., Thomsen et al.
720 2006; Weinberger et al. 2008; Sfriso et al. 2012; this study). Thus, considering: i) this
721 species can bloom in areas previously devoid of native macrophytes, reaching high
722 biomass densities that can lead to the occurrence of summer anoxic events; ii) the
723 future predicted temperatures for Ireland may enhance the growth of *A.*

724 *vermiculophyllum* in Irish estuaries; and iii) the expected increase in the number of
725 estuaries affected by nutrient over-enrichment as consequence of intensification of
726 agriculture in Ireland (Food Wise 2025; https://www.agriculture.gov.ie/2025strategy/);
727 the addition of this species to Irish flora in a global change context could be considered
728 a threat for biodiversity and ecosystem functioning, rather than an opportunity for the
729 recovery of ecosystem functioning.

730
731
732 **References**
733

734 Abreu, M.H., Pereira, R., Sousa-Pinto, I., Yarish, C., 2011. Ecophysiological studies of
735 the non-indigenous species *Gracilaria vermiculophylla* (Rhodophyta) and its
736 abundance patterns in Ria de Aveiro lagoon, Portugal. Eur. J. Phycol. 46, 453–
737 464.
738 Airoldi, L., Beck, M.W., 2007. Loss, status and trends for coastal marine habitats of
739 Europe. Oceanogr. Mar. Biol. An Annu. Rev. 45, 345–405.
740 Anderson, M.J., Gorley, R.N., Clarke, K.R., 2008. PERMANOVA+ for PRIMER: Guide
741 to Software and Statistical Methods. PRIMER-E, Plymouth, UK. p. 204.
742 Andréfouët, S., Muller-Karger, F.E., Hochberg, E.J., Hu, C., Carder, K.L., 2001.
743 Change detection in shallow coral reef environments using Landsat 7 ETM+ data.
744 Remote Sens. Environ. 78, 150–162.
745 Andrew, N., Mapstone, B., 1987. Sampling and the description of spatial pattern in
746 marine ecology. Oceanogr. Mar. Biol. Annu. Rev. 25, 39–90.
747 Baamonde-López, S., Baspino-Fernández, I., Barreiro-Lozano, R., Cremades-Ugarte,
748 J., 2007. Is the cryptic alien seaweed *Ulva pertusa* (Ulvales, Chlorophyta) widely
749 distributed along European Atlantic coasts? Bot. Mar. 50, 267–274.
750 Bermejo, R., Heesch, S., Mac Monagail, M., O'Donnell, M., Daly, E., Wilkes, R.J.,
751 Morrison, L., 2019a. Spatial and temporal variability of biomass and composition
752 of green tides in Ireland. Harmful Algae 81, 94–105.
753 Bermejo, R., Macías, M., Cara, C.L., Sánchez-García, J., Hernández, I., 2019b. Culture
754 of *Chondracanthus teedei* and *Gracilariopsis longissima* in a traditional salina from
755 southern Spain. J. Appl. Phycol. 31, 561–573.
756 Bermejo, R., Ramírez-Romero, E., Vergara, J.J., Hernández, I., 2015. Spatial patterns
757 of macrophyte composition and landscape along the rocky shores of northern
758 coasts of the Alboran Sea. Estuar. Coast. Shelf Sci. 155, 17–28.
759 Burrows, M.T., Harvey, R., Robb, L., Poloczanska, E.S., Mieszkowska, N., Moore, P.,
760 Leaper, R., Hawkins, S.J., Benedetti-Cecchi, L., 2009. Spatial scales of variance
761 in abundance of intertidal species: effects of region, dispersal mode, and trophic
762 level. Ecology 90, 1242–1254.
763 Byers, J.E., Gribben, P.E., Yeager, C., Sotka, E.E., 2012. Impacts of an abundant
764 introduced ecosystem engineer within mudflats of the southeastern US coast.
765 Biol. Invasions 14, 2587–2600.
766 Cacabelos, E., Engelen, A.H., Mejia, A., Arenas, F., 2012. Comparison of the
767 assemblage functioning of estuary systems dominated by the seagrass
768 Nanozostera noltii versus the invasive drift seaweed *Gracilaria vermiculophylla*. J.
769 Sea Res. 72, 99–105.
770 Cardoso, R.S., Mattos, G., Caetano, C.H.S., Cabrini, T.M.B., Galhardo, L.B., Meireis,
771 F., 2012. Effects of environmental gradients on sandy beach macrofauna of a
772 semi-enclosed bay. Mar. Ecol. 33, 106–116.
773 Chappuis, E., Terradas, M., Cefalì, M.E., Mariani, S., Ballesteros, E., 2014. Vertical
774 zonation is the main distribution pattern of littoral assemblages on rocky shores at
775 a regional scale. Estuar. Coast. Shelf Sci. 147, 113–122.

776 Cohen, J., 1960. A coefficient of agreement for nominal scales. Educ. Psychol. Meas.
777 20, 37–46.
778 Costanza, R., d'Arge, R., de Groot, R., Farber, S., Grasso, M., Hannon, B., Limburg,
779 K., Naeem, S., O'Neill, R. V., Paruelo, J., Raskin, R.G., Sutton, P., van den Belt,
780 M., 1997. The value of the world's ecosystem services and natural capital. Nature
781 387, 253–260.
782 Davoult, D., Surget, G., Stiger-Pouvreau, V., Noisette, F., Riera, P., Stagnol, D.,
783 Androuin, T., 2017. Multiple effects of a *Gracilaria vermiculophylla* invasion on
784 estuarine mudflat functioning and diversity. Mar. Environ. Res. 131, 227–235.
785 Dogliotti, A.I., Gossn, J.I., Vanhellemont, Q., Ruddick, K.G., 2018. Detecting and
786 quantifying a massive invasion of floating aquatic plants in the Río de la Plata
787 turbid waters using high spatial resolution ocean color imagery. Remote Sens. 10,
788 1140.
789 Foody, G.M., 1992. Derrivation and applications of probablistic measures of class
790 membership from maximum-likelihood classification. Photogramm. Eng. Remote
791 Sens. 58, 1335-1341.
792 Fort, A., Mannion, C., Fariñas-franco, J.M., Sulpice, R., 2020. Green tides select for
793 fast expanding *Ulva* strains. Sci. Total Environ. 698, 134337.
794 Freshwater, D.W., Rueness, J., 1994. Phylogenetic relationships of some European
795 *Gelidium* (Gelidiales, Rhodophyta) species, based on *rbc*L nucleotide sequence
796 analysis. Phycologia 33, 187–194.
797 Gao, G., Clare, A.S., Rose, C., Caldwell, G.S., 2016. Eutrophication and warming-
798 driven green tides (*Ulva rigida*) are predicted to increase under future climate
799 change scenarios. Mar. Pollut. Bull. 114, 439–447.
800 Gilmore, S., Saleem, A., Dewan, A., 2015. Effectiveness of DOS (Dark-Object
801 Subtraction) method and water index techniques to map wetlands in a rapidly
802 urbanising megacity with Landsat 8 data, in Veenendaal, B. and Kealy, A. (ed),
803 Proceedings of Research@Locate in conjunction with the annual conference on
804 spatial information in Australia and New Zealand, Vol-1323, Mar 10-12 2015, 100-
805 108. Brisbane: CEUR-WS.
806 Gonzalez, D.J., Smyth, A.R., Piehler, M.F., Mcglathery, K.J., 2013. Mats of the
807 nonnative macroalga, *Gracilaria vermiculophylla*, alter net denitrification rates and
808 nutrient fluxes on intertidal mudflats. Limnol. Oceanogr. 58, 2101–2108.
809 Gorelick, N., Hancher, M., Dixon, M., Ilyushchenko, S., Thau, D., Moore, R., 2017.
810 Google Earth Engine: Planetary-scale geospatial analysis for everyone. Remote
811 Sens. Environ. 202, 18-27.
812 Grazia-Corradi, M., Gorbi, G., Zanni, C., 2006. Hypoxia and sulphide influence gamete
813 production in *Ulva* sp. Aquat. Bot. 84, 144–150.
814 Guillemin, M.-L., Akki, S.A., Givernaud, T., Mouradi, A., Valero, M., Destombe, C.,
815 2008. Molecular characterisation and development of rapid molecular methods to
816 identify species of Gracilariaceae from the Atlantic coast of Morocco. Aquat. Bot.
817 89, 324–330.
818 Guiry, M. D., Guiry, G. M., 2019. *AlgaeBase.*, *National University of Ireland*.
819 Gulbransen, D., Mcglathery, K., 2013. Nitrogen transfers mediated by a perennial, non-
820 native macroalga: a 15 N tracer study. Mar. Ecol. Prog. Ser. 482, 299–304.
821 Haram, L.E., Kinney, K.A., Sotka, E.E., Byers, J., 2018. Mixed effects of an introduced
822 ecosystem engineer on the foraging behavior and habitat selection of predators.
823 Ecology 99, 2751–2762.
824 Heesch, S., Broom, J.E.S., Neill, K.F., Farr, T.J., Dalen, J.L., Nelson, W.A., 2009. *Ulva*,
825 *Umbraulva* and *Gemina*: Genetic survey of New Zealand taxa reveals diversity
826 and introduced species. Eur. J. Phycol. 44, 143–154.
827 Heesch, S., Pažoutová, M., Moniz, M.B.J., Rindi, F., 2016. Prasiolales
828 (Trebouxiophyceae, Chlorophyta) of the Svalbard Archipelago: diversity,
829 biogeography and description of the new genera *Prasionella* and *Prasionema*.
830 Eur. J. Phycol. 51, 171–187.

Hu, L., Zeng, K., Hu, C., He, M.X., 2019. On the remote estimation of *Ulva prolifera* areal coverage and biomass. Remote Sens. Environ. 223, 194-207.

Jaspers, C., Møller, L.F., Kiørboe, T., 2011. Salinity gradient of the Baltic Sea limits the reproduction and population expansion of the newly invaded comb jelly *Mnemiopsis leidyi*. PLoS One 6, e24065.

Keller, E.L., Berke, S.K., Needham, C.N., Salerno, C.R., 2019. A Double-Edged Sword: Infaunal Responses to Agarophyton vermiculophyllum in the Mid-Atlantic United States. Estuaries and Coasts 42, 1924–1937.

Kim, S.Y., Weinberger, F., Boo, S.M., 2010. Genetic data hint at a common donor region for invasive atlantic and pacific populations of *Gracilaria vermiculophylla* (Gracilariales, Rhodophyta). J. Phycol. 46, 1346–1349.

Krueger-Hadfield, S.A., Kollars, N.M., Byers, J.E., Greig, T.W., Hammann, M., Murray, D.C., Murren, C.J., Strand, A.E., Terada, R., Weinberger, F., Sotka, E.E., 2016. Invasion of novel habitats uncouples haplo-diplontic life cycles. Mol. Ecol. 25, 3801–3816.

Krueger-Hadfield, S.A., Kollars, N.M., Strand, A.E., Byers, J.E., Shainker, S.J., Terada, R., Greig, T.W., Hammann, M., Murray, D.C., Weinberger, F., Sotka, E.E., 2017a. Genetic identification of source and likely vector of a widespread marine invader. Ecol. Evol. 7, 4432–4447.

Krueger-Hadfield, S.A., Magill, C.L., Bunker, F., Mieszkowska, N., Sotka, E., Maggs, C.A., 2017b. When invaders go unnoticed: the case of *Gracilaria vermiculophylla* in the British Isles. Cryptogamie, Algologie. 38, 379–400.

Krueger-Hadfield, S.A., Stephens, T.A., Ryan, W.H., Heiser, S., 2018. Everywhere you look, everywhere you go, there' s an estuary invaded by the red seaweed *Gracilaria vermiculophylla* (Ohmi) Papenfuss, 1967. Bioinvasions Rec. 7, 343-355.

Kutser, T., Metsamaa, L., Strömbeck, N., Vahtmäe, E., 2006. Monitoring cyanobacterial blooms by satellite remote sensing. Estuar. Coast. Shelf Sci. 67, 303-312.

Lavery, P.S., Lukatelich, R.J., McComb, A.J., 1991. Changes in the biomass and species composition of macroalgae in a eutrophic estuary. Estuar. Coast. Shelf Sci. 33, 1–22.

Lewis, L.J., Davenport, J., Kelly, T.C., 2002. A Study of the Impact of a Pipeline Construction on Estuarine Benthic Invertebrate Communities. Estuar. Coast. Shelf Sci. 55, 213–221.

Lotze, H.K., Lenihan, H.S., Bourque, B.J., Bradbury, R.H., Cooke, R.G., Kay, M.C., Kidwell, S.M., Kirby, M.X., Peterson, C.H., Jackson, J.B.C., 2006. Depletion, degradation, and recovery potential of estuaries and coastal seas. Science 312, 1806–1809.

Louis, J., Debaecker, V., Pflug, B., Main-Knorn, M., Bieniarz, J., Mueller-Wilm, U., Cadau, E., Gascon, F., 2016. Sentinel-2 Sen2Cor: L2A Processor for Users. In Proceedings of the Living Planet Symposium (Spacebooks Online), Prague, Czech Republic, 9–13 May 2016, 1–8.

Lyngby, J.E., Mortensen, S., Ahrensberg, N., 1999. Bioassessment techniques for monitoring of eutrophication and nutrient limitation in coastal ecosystems. Mar. Pollut. Bull. 39, 212–223.

Malta, E.-J., Draisma, S.G.A., Kamermans, P., 1999. Free-floating *Ulva* in the southwest Netherlands: species or morphotypes? A morphological, molecular and ecological comparison. Eur. J. Phycol. 34, 443–454.

Malta, E.-J., Verschuure, J.M., 1997. Effects of environmental variables on between-year variation of *Ulva* growth and biomass in a euthropic brackish lake. J. Sea Res. 38, 71–84.

Mangialajo, L., Chiantore, M., Susini, M.-L., Meinesz, A., Cattaneo-Vietti, R., Thibaut, T., 2012. Zonation patterns and interspecific relationships of fucoids in microtidal environments. J. Exp. Mar. Bio. Ecol. 412, 72–80.

885 Martínez-Garrido, J., Bermejo, R., Serrão, E.A., Sánchez-Lizaso, J., González-
886 Wangüemert, M., 2017. Regional Genetic Structure in the Aquatic Macrophyte
887 *Ruppia cirrhosa* Suggests Dispersal by Waterbirds. Estuaries and Coasts 40,
888 1705-1716,
889 Mineur, F., De Clerck, O., Le Roux, A., Maggs, C.A., Velarque, M., 2010. *Polyopes*
890 *lancifolius* (Halymeniales , Rhodophyta), a new component of the Japanese
891 marine flora introduced to Europe. Phycologia 49, 86–96.
892 Mineur, F., Arenas, F., Assis, J., Davies, A., Engelen, A.H., Fernandes, F., Malta, E.,
893 Thibaut, T., Van Nguyen, T., Vaz-Pinto, F., Vranken, S., Serrão, E. a., De Clerck,
894 O., 2015. European seaweeds under pressure: Consequences for communities
895 and ecosystem functioning. J. Sea Res. 98, 91–108.
896 Mollet, J., Rahaoui, A., Lemoine, Y., 1998. Yield, chemical composition and gel
897 strength of agarocolloids of *Gracilaria gracilis*, *Gracilariopsis longissima* and the
898 newly reported *Gracilaria* cf. *vermiculophylla* from Roscoff (Brittany, France).
899 Jounal Appl. Phycol. 10, 59–66.
900 Muangmai, N., Vo, T.D., Kawaguchi, S., 2014. Seasonal Fluctuation in a Marine Red
901 Alga, *Gracilaria vermiculophylla* (Gracilariales, Rhodophyta), from Nokonoshima
902 Island, Southern Japan. J. Fac. Agric. Kyushu Univ. 59, 243–248.
903 Nejrup, L.B., Pedersen, M.F., 2010. Growth and biomass development of the
904 introduced red alga *Gracilaria vermiculophylla* is unaffected by nutrient limitation
905 and grazing. Aquat. Biol. 10, 249–259.
906 Nelson, T.A., Haberlin, K., Nelson, A. V., Ribarich, H., Hotchkiss, R., Alstyne, K.L. Van,
907 Buckingham, L., Simunds, D.J., Fredrickson, K., 2008. Ecological and
908 physiological controls of species composition in green macroalgal blooms.
909 Ecology 89, 1287–1298.
910 Nyberg, C.D., Wallentinus, I., 2009. Long-term survival of an introduced red alga in
911 adverse conditions Long-term survival of an introduced red alga in adverse
912 conditions. Mar. Biol. Res. 304–308.
913 Nylund GM., Weinberger F., Rempt M., Pohnert G., 2011. Metabolomic assessment of
914 induced and activated chemical defence in the invasive red alga *Gracilaria*
915 *vermiculophylla*. PLoS ONE 6(12):e29359
916 Occhipinti-Ambrogi, A., 2001. Transfer of marine organisms: a challenge to the
917 conservation of coastal biocoenoses. Aquat. Conserv. Mar. Freshw. Ecosyst. 11,
918 243–251.
919 Pedersen, M.F., Borum, J., 1996. Nutrient control of algal growth in estuarine waters.
920 Nutrient limitation and the importance of nitrogen requirements and nitrogen
921 storage among phytoplankton and species of macroalgae. Mar. Ecol. Prog. Ser.
922 142, 261–272.
923 Pedersen, M.F., Johnsen, K.L., 2017. Nutrient (N and P) dynamics of the invasive
924 macroalga *Gracilaria vermiculophylla*: nutrient uptake kinetics and nutrient release
925 through decomposition. Mar. Biol. 164, 1–12.
926 R Development Core Team (2017) R: a language and environment for statistical
927 computing. R Foundation for Statistical Computing, Vienna http://www.R-
928 project.org/
929 Ramus, A.P., Silliman, B.R., Thomsen, M.S., Long, Z.T., 2017. An invasive foundation
930 species enhances multifunctionality in a coastal ecosystem. Proc. Natl. Acad. Sci.
931 U. S. A. 114, 8580–8585.
932 Rempt M., Weinberger F., Grosser K., Phnert G., 2012. Conserved and species-
933 specific oxylipin pathways in the wound-activated chemical defense of the
934 noninvasive red alga *Gracilaria chilensis* and the invasive *Gracilaria*
935 *vermiculophylla*. Beilstein J. Org. Chem. 8:283–289.
936 Robertson, B.P., Savage, C., 2018. Mud-entrained macroalgae utilise porewater and
937 overlying water column nutrients to grow in a eutrophic intertidal estuary.
938 Biogeochemistry 139, 1–16.
939 Rueness, J., 2005. Life history and molecular sequences of *Gracilaria vermiculophylla*

(Gracilariales, Rhodophyta), a new introduction to European waters. Phycologia 44, 120–128.
Schories, D., Reise, K., 1993. Germination and anchorage of *Enteromorpha* spp. in sediments of the Wadden Sea. Helgoländer Meeresuntersuchungen 47, 275–285.
Sfriso, A., Facca, C., Ghetti, P.F., 2003. Temporal and spatial changes of macroalgae and phytoplankton in a Mediterranean coastal area: The Venice lagoon as a case study. Mar. Environ. Res. 56, 617–636.
Sfriso, A., Wolf, M.A., Maistro, S., Sciuto, K., Moro, I., 2012. Spreading and autoecology of the invasive species *Gracilaria vermiculophylla* (Gracilariales, Rhodophyta) in the lagoons of the north-western Adriatic Sea (Mediterranean Sea, Italy). Estuar. Coast. Shelf Sci. 114, 192–198.
Smetacek, V., Zingone, A., 2013. Green and golden seaweed tides on the rise. Nature 504, 84–8.
Sotka, E.E., Baumgardner, A.W., Bippus, P.M., Destombe, C., Duermit, E.A., Endo, H., Flanagan, B.A., Kamiya, M., Lees, L.E., Murren, C.J., Nakaoka, M., Shainker, S.J., Strand, A.E., Terada, R., Valero, M., Weinberger, F., Krueger-hadfield, S.A., 2018. Combining niche shift and population genetic analyses predicts rapid phenotypic evolution during invasion. Evol. Appl. 11, 781–793.
Steentoft, M., Irvine, L.M., Farnham, W.F., 1995. Two terete species of *Gracilaria* and *Gracilariopsis* (Gracilariales, Rhodophyta) in Britain. Phycologia 34, 113–127.
Strickland JD, Parsons TR (1968) A practical handbook of seawater analysis. Bull. Fish. Res. Board Can., No, p 167.
Surget, G., Le Lann, K., Delebecq, G., Kervarec, N., Donval, A., Poullaouec, M.-A., Bihannic, I., Poupart, N., Stiger-Pouvreau, V., 2017. Seasonal phenology and metabolomics of the introduced red macroalga *Gracilaria vermiculophylla,* monitored in the Bay of Brest (France). J. Appl. Phycol. 29, 2651–2666.
Sverdrup, H.U., 1953. On Conditions for the Vernal Blooming of Phytoplankton. J. du Cons. Perm. Int. pour l'Exploration la Mer 18, 287–295.
Teichberg, M., Fox, S.E., Olsen, Y.S., Valiela, I., Martinetto, P., Iribarne, O., Muto, E.Y., Petti, M.A. V, Corbisier, T.N., Soto-Jiménez, M., Páez-Osuna, F., Castro, P., Freitas, H., Zitelli, A., Cardinaletti, M., Tagliapietra, D., 2010. Eutrophication and macroalgal blooms in temperate and tropical coastal waters: Nutrient enrichment experiments with *Ulva* spp. Glob. Chang. Biol. 16, 2624–2637.
Thomsen, M.S., McGlathery, K.J., Tyler, A.C., 2006. Macroalgal Distribution Patterns in a Shallow, Soft-bottom Lagoon, with Emphasis on the Nonnative *Gracilaria vermiculophylla* and *Codium fragile*. Estuaries and Coasts 29, 465–473.
Thomsen MS, McGlathery KJ (2007) Stress tolerance of the invasive macroalgae *Codium fragile* and *Gracilaria vermiculophylla* in a soft-bottom turbid lagoon. Biol. Invasions 9:499–513.
Thomsen, M.S., Stæhr, P.A., Nejrup, L.B., Schiel D.R., 2013 Effects of the invasive macroalgae *Gracilaria vermiculophylla* on two co-occurring foundation species and associated invertebrates. Aquat. Invasions 8:133–145.
Valiela, I., Mcclelland, J., Hauxwell, J., Behr, P.J., Hersh, D., Foreman, K., 1997. Macroalgal blooms in shallow estuaries: Controls and ecophysiological and ecosystem consequences. Limnol. Oceanogr. 42, 1105–1118.
Vermaat, J.E., Sand-Jensen, K., 1987. Survival, metabolism and growth of *Ulva lactuca* under winter conditions: a laboratory study of bottlenecks in the life cycle. Mar. Biol. 95, 55–61.
Villares, R., Carballeira, A., 2004. Nutrient Limitation in Macroalgae (*Ulva* and *Enteromorpha*) from the Rías Baixas (NW Spain). Mar. Ecol. 25, 225–243.
Vincent, R.K., Qin, X., McKay, R.M.L., Miner, J., Czajkowski, K., Savino, J., Bridgeman, T., 2004. Phycocyanin detection from LANDSAT TM data for mapping cyanobacterial blooms in Lake Erie. Remote Sens. Environ. 83, 381-392.
Wan, A.H.L., Wilkes, R.J., Heesch, S., Bermejo, R., Johnson, M.P., Morrison, L., 2017. Assessment and characterisation of Ireland's green tides (*Ulva* species). PLoS

One 12, e0169049.
Weinberger, F., Buchholz, B., Karez, R., Wahl, M., 2008. The invasive red alga *Gracilaria vermiculophylla* in the Baltic Sea: adaptation to brackish water may compensate for light limitation. Aquat. Biol. 3, 251–264.
Wright, Jeffrey T., James E. Byers, Jayna L. DeVore, and Erik E. Sotka. 2014. Engineering or food? Mechanisms offacilitation by a habitat- forming invasive seaweed. Ecology 95 (10): 2699–2706.
Xing, Q., Guo, R., Wu, L., An, D., Cong, M., Qin, S., Li, X., 2017. High-Resolution Satellite Observations of a New Hazard of Golden Tides Caused by Floating *Sargassum* in Winter in the Yellow Sea. IEEE Geosci. Remote Sens. Lett. 14, 1815-1819.
Yabe, T., Ishii, Æ.Y., Amano, Æ.Y., Koga, T., Hayashi, Æ.S., Nohara, Æ.S., 2009. Green tide formed by free-floating *Ulva* spp. at Yatsu tidal flat, Japan. Limnology 10, 239–245.
Yokoya, N.S., Kakita, H., Obika, H., Kitamura, T., 1999. Effects of environmental factors and plant growth regulators on growth of the red alga *Gracilaria vermiculophylla* from Shikoku Island, Japan. Hydrobiologia 398/399, 339–347.
Yoshida, G., Uchimura, M., Hiraoka, M., 2015. Persistent occurrence of floating *Ulva* green tide in Hiroshima Bay, Japan: seasonal succession and growth patterns of *Ulva pertusa* and *Ulva* spp. (Chlorophyta, Ulvales). Hydrobiologia 758, 223–233.
Zhang, J., Shi, J., Gao, S., Huo, Y., Cui, J., Shen, H., Liu, G. & He, P., 2019. Annual patterns of macroalgal blooms in the Yellow Sea during 2007–2017. PLoS One 14, e0210460.

Fig. 1.- Geographical location of the Clonakilty estuary in Ireland (a). Map of the Clonakilty showing the location of the wastewater treatment plant (black triangle) inner and outer sections (black squares) (b). Detailed maps outlining a schematic representation of the spatial sampling design in the inner (c) and outer sections (d). Black dots represent seaweed sampling station, and black "x" seawater sampling stations in subfigures c and d.

Fig. 2. Potential extension for *Agarophyton* and *Ulva*, and the overlapping between both, in the Clonakilty estuary based on satellite imagery collected from 2010 to 2018.

Fig. 3.- Biomass (wet wt.) (n =54) of *A. vermiculophyllum* for each section over seven different sampling occasions (a). Biomass (wet wt.) of *A. vermiculophyllum* for each site (Sites 1 and 3, n =126; Sites 2 and 4, n =63) and position in the seaweed bloom (b). Box plots indicate the mean (bold +), the median (bold line inside the box), the first and third quartile (upper and lower lines defining the box), the extreme values whose distance from the box is at most 1.5 times the interquartile range (whiskers), and remaining outliers (dark dots). Box plots marked by the same letter are not significantly different according to post hoc analyses. In figure b, the different colours of the letters over the bars indicate that post hoc comparisons between positions were performed within each one of the four sites.

Fig. 4.- Mean tissue N (above) and P (below) content of *A. vermiculophyllum* for each sampling occasion. Lower and Upper error bars represent standard deviation (n = 6). Bars marked by the same letter are not significantly different according to post hoc analyses. In figure b, the different colours of the letters over the bars indicate that post hoc comparisons between sampling occasions were performed within each one of the two sections.

Fig. 5.- Score biplot of the first and second principal component based on biomass (Bio), tissue N (%N) and P (%P) contents, and tissue N:P (N:P) ratio (red arrows) of *Agarophyton* bloom for the four sampling sites studied and six of the seven sampling occasions (August 2016 - light red dots; October 2016 - grey dots; February 2017 - white dots; April 2017 - green dots; June 2017 - yellow dots; August 2017 - dark red dots). Blue arrows represent environmental variables fitted using "envfit" function of the Vegan package in R (accumulated rainfall - Rain; dissolved inorganic nitrogen - DIN; dissolved inorganic phosphorous - DIP; maximum temperature - Max; minimum temperature - Min; salinity - Sal; solar radiation - Rad).

Sampling	Rain (mm)	Max (ºC)	Min (ºC)	Rad (J cm^{-2})
Jul 16	40.3	18.2	10.2	1587.0
Aug 16	25.7	24.6	12.6	1274.7
Oct 16	5.3	16.3	4.3	999.1
Feb 17	24.0	12.5	5.6	401.2
Apr 17	6.9	12.3	2.0	1093.6
Jun 17	16.3	26.0	5.4	1821.9
Aug 17	35.6	17.8	10.1	1487.4

Table 1- Meteorological parameters for the Clonakilty estuary: Accumulated rainfall (Rain); Maximum (Max) and Minimum (Min) air temperatures during the week previous to the sampling occasion; and mean global radiation (Rad).

Site	Sampling	NO_2^- (µM)	NO_3^- (µM)	NH_4^+ (µM)	DIN (µM)	DIP (µM)	Sal (PSU)
Inner 1	Aug 16	2.02	52.14	29.29	82.86	0.84	18.2
	Oct 16	2.00	140.00	7.14	148.57	0.76	33.0
	Feb 17	2.29	273.57	10.00	285.71	0.60	12.8
	Apr 17	0.55	112.86	3.57	117.14	0.65	32.3
	Jun 17	0.55	135.71	3.57	140.00	1.02	5.0
	Aug 17	3.86	61.43	17.14	82.14	1.99	12.0
Inner 2	Aug 16	1.79	40.00	15.71	57.86	0.55	11.5
	Oct 16	2.14	187.14	10.00	199.29	1.12	30.0
	Feb 17	2.00	147.86	7.14	157.14	0.37	19.0
	Apr 17	0.52	98.57	6.43	105.00	0.64	31.0
	Jun 17	1.07	92.14	11.43	104.29	1.14	6.1
	Aug 17	0.74	17.14	8.57	26.43	1.63	29.0
Outer 1	Aug 16	1.55	18.57	4.29	24.29	0.32	24.5
	Oct 16	1.60	138.57	2.86	142.86	0.37	25.8
	Feb 17	1.64	61.43	4.29	67.14	0.28	29.0
	Apr 17	0.00	26.43	1.43	28.57	0.16	32.0
	Jun 17	1.00	77.86	6.43	85.00	0.89	10.2
	Aug 17	0.91	96.43	1.43	99.29	0.97	8.0
Outer 2	Aug 16	1.64	75.00	5.71	82.14	0.33	14.1
	Oct 16	1.74	102.86	5.00	110.00	0.31	33.2
	Feb 17	2.17	39.29	7.14	48.57	1.54	30.1
	Apr 17	0.00	10.00	0.00	10.00	0.23	33.0
	Jun 17	0.88	62.14	7.86	70.71	1.13	19.6
	Aug 17	1.29	43.57	10.00	55.00	0.75	20.0

Table 2- Mean values of nutrient concentrations (NO_2^- - Nitrite; NO_3^- - Nitrate; NH_4^+ - ammonia; DIN - Dissolved Inorganic Nitrogen; DIP - Dissolved inorganic phosphorus) and salinity (Sal) for each Site and Sampling occasion.

Sensor	Year	Month	Accuracy	Kappa	*Ulva* (ha)	*Agarophyton* (ha)	Overlapping (ha)
Landsat-7 ETM+	2010	June	99.29%	0.9329	46.1	0	0
Landsat-7 ETM+	2011	-	-	-	-	-	-
Landsat-7 ETM+	2012	September	98.97%	0.9524	32.5	0	0
Landsat-7 ETM+	2013	April	98.41%	0.8643	19.6	0	0
Landsat-7 ETM+	2014	July	98.45%	0.8304	31.5	3.9	2.4
Sentinel-2	2015	August	97.42%	0.8908	50.8	3.7	0.6
Sentinel-2	2016	August	97.48%	0.8375	27.7	4.5	1.2
Sentinel-2	2017	July	87.26%	0.7317	26.7	5.5	2.4
Sentinel-2	2018	July	98.05%	0.9617	35.6	8.1	2.7
Potential extension					**63.1**	**9.9**	**3.2**

Table 3- Classification accuracy, Kappa coefficient, *Ulva* and *Agarophyton* extension from 2010 to 2018, potential extension of both *Ulva* and *Agarophyton* considering this 8-year period, and overlapping between *Agarophyton* and the potential extension of *Ulva*.

Source	df	MS(x10^5)	Ps-F
Sampling occasion (SO)	**6**	**204.50**	**19.59*** **
Area (A)	**1**	**112.99**	**10.83** **
Position (Po)	**2**	**61.78**	**7.01** **
SOxA	6	28.59	2.74
SOxPo	12	12.20	1.38
AxPo	**2**	**55.24**	**6.27** **
Site (Si(SOxA))	**14**	**10.44**	**2.52***
SOxAxPo	12	16.76	1.90
PoxSi(SOxA)	**28**	**8.81**	**2.13***
Station(PoxSi(SOxA))	42	4.14	1.42
Residual	252	2.91	
Total	377		

Table 4- Results of five-way PERMANOVA analysis testing the effects of the factors "Sampling Occasion" (SO - fixed, 7 levels), "Position in the bloom" (Po - fixed, 3 levels), "Area" (A - fixe, 2 levels), "Site" (Si - Random nested in "AxSO"), and "Sampling Station" (Station- Random nested in "SixPo") on the biomass of *A. vermiculophyllum* in the Clonakilty estuary. * p-value < 0.05; ** p-value < 0.01; *** p-value < 0.001.

		%N		%P	
	df	**MS**	**F**	**MS**	**F**
Area (A)	1	0.003	0.02	0.0002	0.43
Sampling occasion (SO)	6	4.753	**24.42*** **	0.0086	**13.15*** **
AxSO	6	0.101	0.52	0.0021	**3.18***
Residuals	28	0.195		0.0006	

Table 5- Results of two-way ANOVA analyses testing the effects of the factors "Sampling Occasion" (SO - fixed, 7 levels) and "Area" (A - fixe, 2 levels) on the tissue N and P content of *A. vermiculophyllum*. * p-value < 0.05; ** p-value < 0.01; *** p-value < 0.001.

	Bio	%N	%P	N:P
DIN	-0.39	**0.44***	0.30	0.12
DIP	0.33	-0.37	-0.04	-0.09
Sal	**-0.55****	0.37	0.09	0.27
Rain	0.24	-0.03	0.09	-0.10
Max	**0.75*****	**-0.59****	0.04	**-0.51***
Min	**0.86*****	**-0.74*****	-0.16	**-0.44***
Rad	**0.74*****	**-0.86*****	**-0.61****	-0.01

Table 6- Spearman correlations (Rho) between environmental and biotic variables. DIN - Dissolved Inorganic Nitrogen; DIP - Dissolved Inorganic Phosphorous; Sal - Salinity; Rain - Accumulated rainfall; Max - Maximum Air Temperature; Min - Minimum Air Temperature; Rad - Global radiation; Bio - Biomass; %N - tissue N content; %P - tissue P content; N:P - tissue N:P ratio. * p-value < 0.05; ** p-value < 0.01; *** p-value < 0.001.

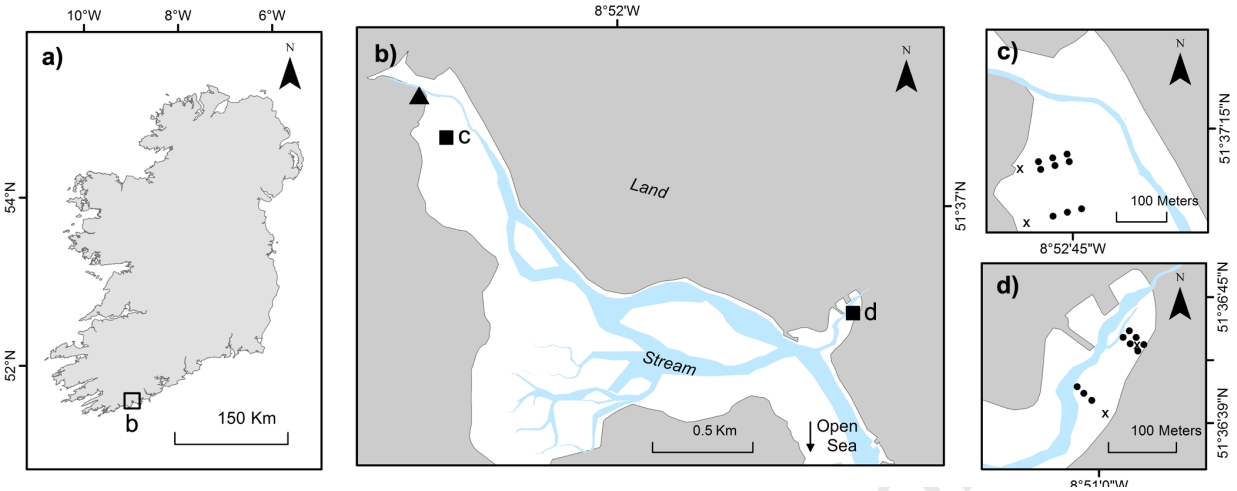

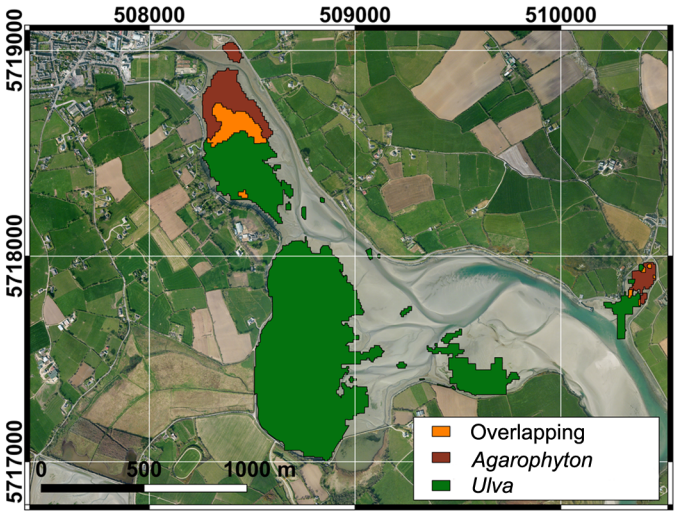

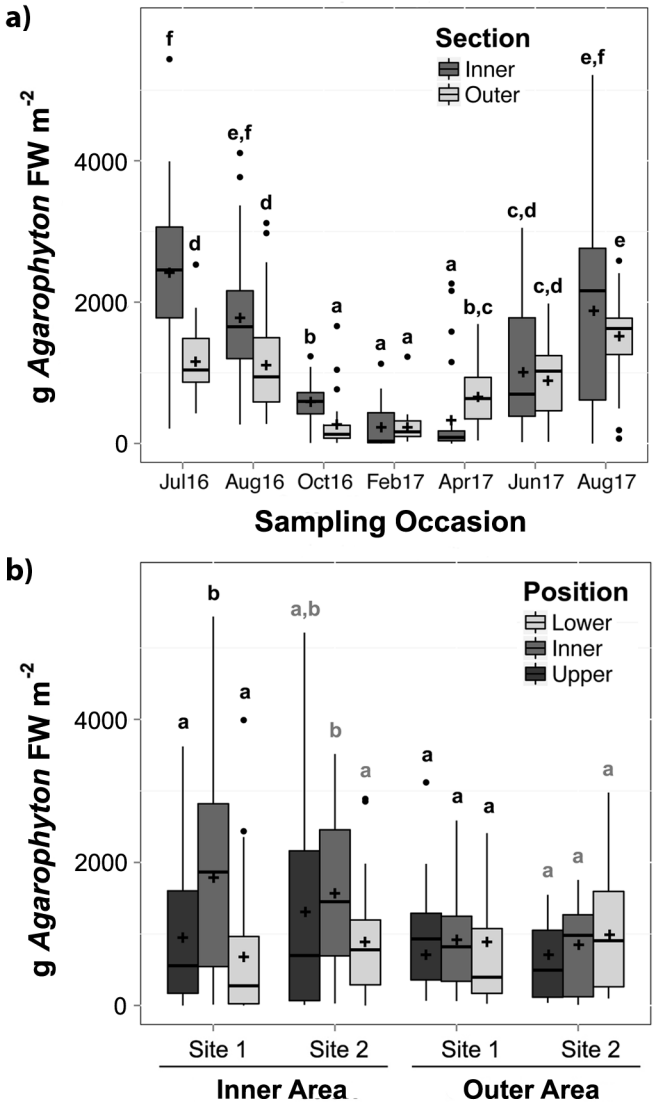
a)
Section
Inner
Outer
g Agarophyton FW m-2
4000
2000
0
f
d
e,f
d
b
a
a
a
a
b,c
c,d
c,d
e,f
e
Jul16
Aug16
Oct16
Feb17
Apr17
Jun17
Aug17
Sampling Occasion
b)
Position
Lower
Inner
Upper
g Agarophyton FW m-2
4000
2000
0
a
b
a
a,b
b
a
a
a
a
a
a
a
a
Site 1
Site 2
Site 1
Site 2
Inner Area
Outer Area

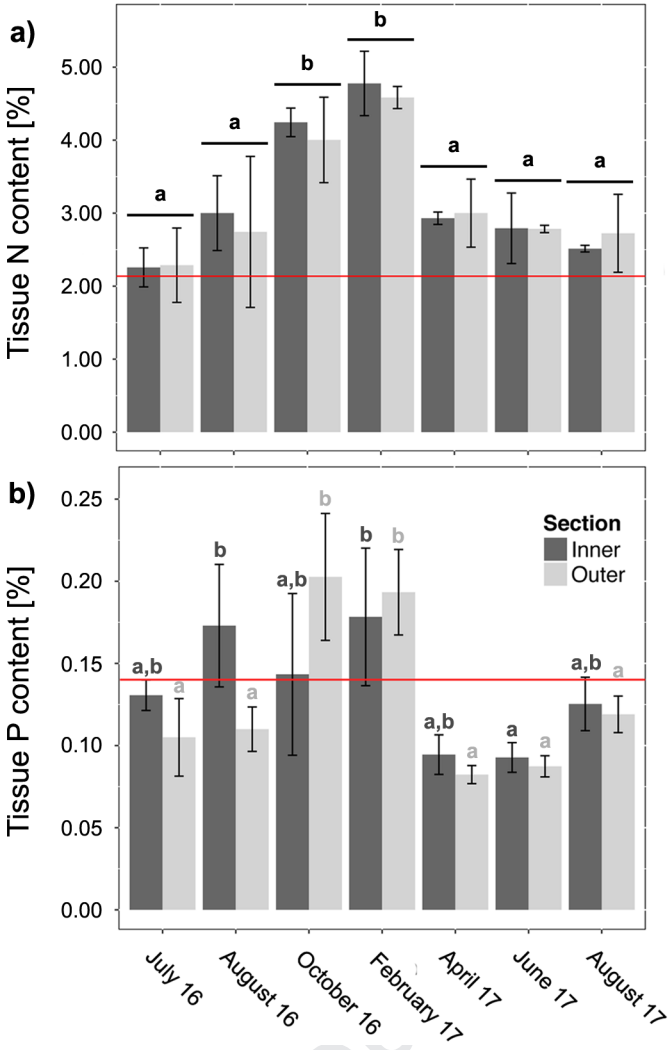

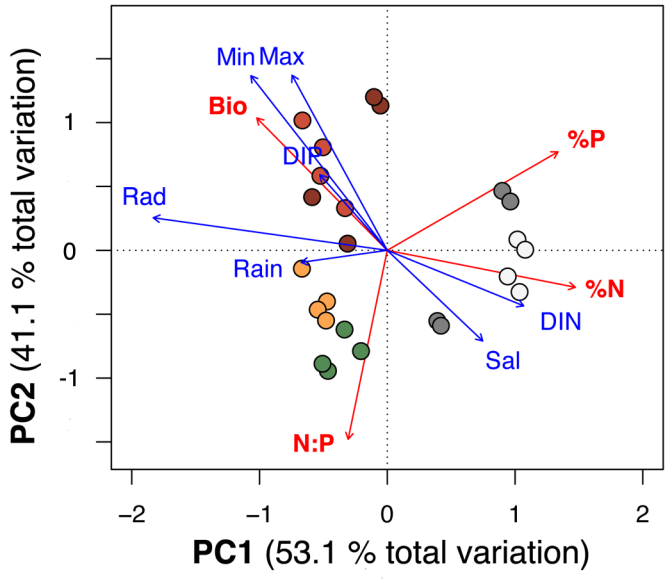

Highlights:

- The presence of *A. vermiculophyllum* is confirmed for the Republic of Ireland.
- Bloom development is constrained by P, not N limitation.
- This alien species can bloom in areas where native bloom forming species cannot.
- Free satellite imagery can be used to reconstruct *A. vermiculophyllum* invasion.
- Biomass followed a seasonal pattern, with peak bloom occurring in summer.

Declaration of interests

☒ The authors declare that they have no known competing financial interests or personal relationships that could have appeared to influence the work reported in this paper.

The authors declare the following financial interests/personal relationships which may be considered as potential competing interests:

N/A